Electro-thermally driven microgrippers for micro-electro-mechanical systems applications

Bordatchev, Evgueni V.; Nikumb, Suwas K.

Publisher's version / Version de l'éditeur:
https://doi.org/10.1117/1.1899312
Journal of Micro/Nanolithography, MEMS, and MOEMS, 4, 4, 2005-05-13

Electro-Thermally Driven Microgrippers for MEMS Applications

Evgueni V. Bordatchev and Suwas K. Nikumb

Integrated Manufacturing Technologies Institute

National Research Council of Canada

London, Ontario, Canada

June 2004

Submitted to: Journal of Microlithography, Microfabrication, and Microsystems

For correspondence:

Evgueni V. Bordatchev, Ph.D., D.Sc., Prof.

Integrated Manufacturing Technologies Institute

National Research Council of Canada

800 Collip Circle, London, ON, Canada, N6G 4X8

Tel: (519) 430-7107

Fax: (519) 430-7064

E-mail: evgueni.bordatchev@nrc-cnrc.gc.ca

Electro-Thermally Driven Microgrippers for MEMS Applications

Evgueni V. Bordatchev and Suwas K. Nikumb

Integrated Manufacturing Technologies Institute, National Research Council of Canada

London, Ontario, Canada

ABSTRACT

This paper presents design, fabrication and performance testing of an innovative, laser machined structure to act as a microgripper. The proposed design constitutes of a pair of identical, cascaded actuation structures oriented in a face-to-face direction, to act as microtweezers. Each microactuator consists of five actuation units joined together horizontally in a consecutive order to build the cascaded structure. The actuation unit incorporates an internal constrainer and two semi-circular-shaped actuation beams. The actuation principle is based on the electro-thermal effect. On application of electrical potential at the back ends, the conductive, geometrically complex structure of the microgripper produces non-uniform resistive heating and uneven thermal expansion generating tweezing displacements and force through a cumulative effect of all the individual actuation units within the cascaded microactuators. High-precision laser micromachining process was employed in the fabrication of the copper and nickel-based prototype microgrippers with overall dimension of 1.4*mm*(L)x2.8*mm*(W) and with relative accuracy within 1%. The geometrical parameters of the prototypes were evaluated in terms of accuracy and precision to demonstrate the fabrication capabilities. Challenges involved and the solutions to develop functional microparts with high aspect ratio (dimensional) with respect to the local elements and overall dimensions were described. The performance of the two microgripper prototypes was analyzed and compared. These microgrippers are useful in micromanipulating and microhandling operations for MEMS, biological, medical, chemical and electro-opto-mechanical engineering applications.

KEYWORDS

microgripper, electro-thermally driven, design, laser microfabrication, performance testing, MEMS

1. INTRODUCTION

Microrobotics and microassembly technologies employed in the development, fabrication and assembly of the micro-electro and micro-opto-electro-mechanical systems (MEMS/MOEMS), often require the use of a microgripper as an end grasping tool for assembly, handling/holding and manipulating micron-size objects such as, tiny mechanical parts, electrical components, biological cells, bacterium, *etc*, without damage or destruction. In such systems, a typical microgripper design consists of a stationary actuator(s) and at least two movable jaws. The operating principle of tweezing/grasping mechanism of the microgripper is based on the specific type of a microactuation principle used in its design. The microactuator is an essential design component of the microgripper that provides the required grasping actions of tweezing jaws and generates the applied force so that the device operates as a gripper or tweezers. Although various actuation methods have been reported in the literature [1-3], the actuations based on electrostatic, thermoelectric, piezoelectric, and shape memory alloy effects are more extensively studied for MEMS/MOEMS applications. In electrostatic microactuators/grippers [4-7], high voltage (up to 250 V) is applied to the electrodes located on gripping arms to generate an electrostatic force between the oppositely charged electrodes to move the tweezing jaws. Unfortunately, the electrostatic actuators produce relatively small force and displacement and require higher driving voltages. To improve the dynamic performance of the electrostatic actuators, a comb-type design [8-9] was used to reduce the driving voltage and to increase or maintain the desired electrostatic force and tweezing displacement. Ideal microgripper performance requires quasi-static motions to grasp and hold an object that may be inappropriate for the electrostatic actuators, which are more suitable for generating vibrating motions. Electro-thermally driven actuators [10-17] are more compact, can provide higher output force and larger displacements, but geometrically are more complex in nature. Actuation motions are generated by application of an electric potential to the conducting elastic material (usually metal) to produce Joule heating (resistive heating) resulting in thermal expansion of the entire structure. Therefore, a complex design and geometry is required to direct the thermal expansion into the desired direction of motion by creating non-uniform resistive heating. Recently, applications of shape-memory alloys (SMA) in combination with electro-thermal actuation were extensively studied [18-23]. SMA materials such as NiTi, NiAl, FePb etc, have significant advantages over metals, such as returning a predetermined shape with substantial recovery force and providing larger deformations at relatively low temperatures.

The successful development of a microgripper or microactuator as any miniature functional component or MEMS/MOEMS devices, is based on the consideration of the framework of the five interrelated fundamental components, which include area of application, principle of actuation, structure design, material to be used, and the fabrication method. These interrelated components create a complex paradigm as shown in Figure 1. The area of application limits the choice of materials to be used, which influences the choice of actuation principle, structure design and fabrication technique, and determines the constraints on the proposed fabrication technology to achieve the desired geometrical quality in terms of accuracy, precision and surface quality. Modern silicon-based surface and bulk micromachining techniques are very efficient for the fabrication of electro-statically and electro-thermally driven microgrippers/actuators due to good line width control and high compatibility with CMOS processing [1]. However, these technologies are not suitable for fabrication of metal, piezoelectric and SMA-based micro-grippers/actuators, particularly, for the fabrication in the range of hundreds of microns and are also expensive for small quantities and prototype fabrication. Several different non-silicon-based micromachining processes, such as, sputtering [24] and sol-gel methods [25], were developed for piezoelectric microstructures fabrication and for deposition of thin films of piezoelectric materials. Also, thicker piezoelectric microstructures fabricated by the slurry casting methods and up to several hundreds of micrometers with lateral dimension control of tens of micrometers were reported [26,27]. On the other hand, the ultra-precision laser fabrication technology can be a cost-effective alternative due to its unique ability to machine a wide range of the light absorbing materials and to fabrication precision miniature parts with complex 2D/3D geometries [11,17,28-30].

This paper presents the design, fabrication and performance testing of a new and innovative structure to act as a microgripper for MEMS/MOEMS, microrobotics, and microassembly applications. In the first part, the overall design, design of the individual actuation unit, challenges in high-precision laser microfabrication and solution methods are discussed. Later, results of the geometry evaluation, dynamic and comparative performance testing of copper and nickel-based prototype microgrippers are presented.

2. DESIGN

Figure 2 illustrates the conceptual design of the microgripper. This is a monolithic structure which does not require post-machining assembly. The design is based on a multi-cascaded approach [16,17] and consists of a pair of identical cascaded actuation structures (microactuators) oriented in a face-to-face direction to act as microtweezers. Tweeze jaws are supported by vertical levers with fixed ends (anchor 2) to hold the object. Each microactuator consists of five actuation units joined horizontally in a consecutive order to build the cascaded structure and is supported by a fixed pillar (anchors 1 and 3) on the outer side. The actuation principle is based on the electro-thermal effect. On application of electrical potential, the conductive structure of the microgripper produces Joule heating and thermal expansion of all the design elements and eventually the entire structure. Actuation units expand with respect to the supporting pillars because of significant differences in the geometrical parameters, such as width and length, and therefore the electric resistance. Proposed design has advantages over other actuator and microgripper designs [11-15, 18-23] due to cumulative effect in generating output displacement and force. Each actuation unit generates individual displacement and force that accumulated further by cascaded structures of the microactuator. This advantage allows optimization of required output displacement and force by adjusting a number of actuation units and parallel cascades.

A schematic diagram of the basic actuation unit is shown in Figure 3. It consists of a geometrical combination of a constrainer and two semi-circular-shaped actuation beams. The key function of the actuation unit design is to direct the primary thermal expansion in the desired direction. In the present case, horizontal motions are generated as a result of non-uniform resistive heating. Since the thin, long actuation beam dimensions are 25 μm x 25 μm (width to thickness) in cross-section, they have higher electrical resistance per length unit and heat up more than the wider constrainer with cross-section of 50 μm x 25 μm and relatively lower electrical resistance per length unit.

As a result, the actuation beam expands much more than the constrainer during the electro-thermal heating stage. When the actuation unit is electrically heated, actuation beams tend to expand in all directions evenly. However, the constrainer expands less than the actuation beams because there is no current flow through the constrainer due to no difference of electric potentials between ends of the constrainer. The thermal expansion of the constrainer is caused by only heat propagation from actuation beams due to symmetrical structure of the actuation unit. This limits the expansion of the actuation unit in the vertical direction and directs the primary displacements in the desired horizontal direction, as illustrated in Figure 3.

Figure 4 shows the final geometrical design of the microgripper with overall dimensions of 1.4 (L) x 2.8 (W) *mm*. The complexity of the design involves a combination of design elements with high dimensional aspect ratios between the individual elements and the overall dimensions. For example, a minimal dimension in the microgripper design is 25 μm width of the actuation beam compared to the 2.8 *mm* width of the entire microgripper for a dimensional aspect ratio of 1:112. This design complexity poses key challenges for laser microfabrication of the entire microgripper, which will be discussed in section 4.

3. LASER MICROMACHINING SYSTEM

Figure 5 shows the schematic of the laser micromachining system, which was used for microfabrication of the microgripper prototypes. The system was equipped with a Q-switched diode pumped solid state $Nd:YVO_4$ laser with an appropriate beam delivery system and a three-axis CNC-based motion control system. The laser operates at a wavelength of 1064 *nm* with pulse-to-pulse energy stability of less than 1% *rms* for linear polarization in the TEM_{00} mode. An in-house designed beam delivery system, composed of a combination of beam expander and focusing objective, was used to focus the laser beam on to the workpiece surface. The motion system consisted of a granite base fitted with precision translation stages for X and Y movements with a rated positioning accuracy in the order of 0.5 µm in the X and Y axis. Both the laser and the motion system were controlled and synchronized in time and space using an in-house developed software, which enabled the set up of the process parameters and desired toolpath geometry to achieve required accuracy and precision. Thin foils of copper and nickel with thickness of 25 *µm* and 12.5 *µm* respectively were used for the fabrication of microgripper prototypes. A vacuum fixture, located on the top of the XY translation stage, equipped with a fine control valve, was designed and used to hold the foil flat and precisely at the focal point of the laser beam. The fixture was also helped to remove any surface distortions, striations or unevenness while loading. An optical microscope "Olympus" (model PMG3) and VisionGauge® software were used to measure the geometry of the fabricated prototypes within an accuracy of 0.1 *µm*. All the laser energy/power measurements were carried out using a calibrated laser power meter (model: TMP-300 from Gentec Inc).

4. CHALLENGES IN LASER MICROFABRICATION

During the direct-write laser machining process, laser pulses were applied according to the prescribed toolpath trajectory for material removal. A single laser pulse creates a crater (dent) on the surface removing a certain quantity of material from the workpiece, where the feature characteristics, geometry and the volume of material removed depend on the material properties and the laser parameters [28-32]. The final geometry of the laser-machined part is a result of a sequence of craters conformed in accordance with the predetermined tool path into the workpiece surface. However, laser-machining experiments indicate that the geometry and surface profile of the machined part are not the only defining toolpath parameters but the process is also influenced by the dynamic processes associated within the entire laser machining system and with laser-material interactions. For example:

a) dynamics of the motion control system, particularly, overshooting and acceleration/deceleration of the stages form uneven feed motions during material removal affecting the synchronization with respect to the individual laser beam impulses [17,33,34],
b) dynamic and kinematic disturbances within the entire motion system that cause positional and contour errors in the actual toolpath trajectory and therefore form geometric errors and inaccuracies within the final machined parts [35],
c) dynamic variations within the laser beam parameters, such as, pulse energy, duration, jitter etc., during the laser-material interactions causing changes in the machined surface profile [36,37].

Therefore, only a proper combination and synchronization of motions and laser pulses in time and space supported by optimal processing parameters provides desired geometric accuracy, precision and surface quality [38].

Figure 6 summarizes the challenges in the laser microfabrication of the prototype microgripper with respect to the desired geometry. Two major fabrication issues were resolved: a) the over/undercuts and b) asynchronization of the laser on/off events, desired geometry and actual motions. The source of over/undercutting is the dynamic (also known as contour or following) errors due to poor dynamic performance of the motion system in agile situations. The design of the microgripper involves a significant number of the angular and corner elements, and therefore high-precision feature machining requires a sequential combination of short-distance and long-distance agile movements at a constant speed. In this situation, the inertia of relatively heavy XY translation table creates significant dynamic positioning errors especially in the locations where it is necessary to change direction of motions abruptly, (e.g. corners). In order to achieve higher level of accuracy and precision of the fabricated prototypes, it was necessary to take into account these dynamic errors because sometimes the error magnitudes reached dimensions equivalent to the local design elements (ex. actuation beam width). The solution from conventional machining (e.g. in milling operation, while a cutting tool rotates, stop motions at a certain point, change direction, and continue movement), is not suitable during high-precision laser machining, simply because the laser will continue to fire pulses causing unnecessary material removal and additional heating of the workpiece. In general, during laser processing, cavities at the start and at the end points of motions have been reported due to the acceleration and deceleration of motions [17,33,34]. During these time segments, consecutive laser pulses were located very close to each other, and therefore the workpiece material absorbs more laser energy per square unit, resulting in large amount of material removal. This is because lack of synchronization between the motion and laser pulses to provide a constant overlap between each of the consecutive pulses. Also, the accuracy of corners was highly dependent on the proper synchronization of motions with respect to part geometry. Conventional CAD/CAM systems do not provide advanced options to correct this issue. In the present experiments, proper use of blending options for a given motion controller with respect to dynamics of motion was utilized in order to obtain the desired corner accuracy.

The second issue deals with the asynchronization of the laser-on/off events and individual motions, when motion control turns laser on/off before or after the desired position. Some motion controllers offer advanced features, such as a "look-and-calculate ahead" feature. However, an improper use of this feature could cause asynchronization of laser-on/off events and motions in space and time with respect to the desired geometry leading to errors in the tool path trajectory and final part geometry. As shown in Figure 6, in case of asynchronization, the laser is turned on ahead of the desired time and space location resulting in wrong and incorrect cutting. Proper programming of the toolpath trajectory and the use of the blending options to delay/advance execution of consecutive laser on/off events until the motion was completed resolved this situation. In addition, the laser by itself is an inertial opto-mechatronic system including a method to turn it on/off, e.g. by using an electro-mechanical relay, which requires on/off switching time that could also be considered during high precision machining.

Process parameters, such as, a pulse energy, feed rate and pulse repetition rate, were optimized as described elsewhere [30,34].

5. GEOMETRY EVALUATION

Figure 7 shows the nickel-based microgripper prototype fabricated by direct-writing laser micromachining technique. Table 1 summarizes the dimensional accuracy of the fabricated prototypes in terms of desired/machined dimensions and absolute/relative accuracy (error). Also, all dimensions presented in Table 1 were classified by a specific type of machining operation such as (a) a single cut, (b) a set of consecutive cuts, and (c) a set of non-consecutive cuts. A single cut is a motion within laser on-off time period. A set of consecutive cuts is a combination of consecutive motions that do not involve agile change of motion directions between laser on/off events. A set of non-consecutive cuts is a combination of several single cuts with distinctive directions of motions. The highest accuracy and precision have been achieved in the length dimensions of the constrainer (150.0 *μm)*, the width of the tweezing jaw (50.0 *μm*), the distance between vertical levers (200.0 *μm*) *etc,* which were formed using single cut and consecutive cuts. In these cases, motions were smooth with relatively constant actual velocity and do not have sharp corners and agile movements, and therefore motion system kept the dynamic contour error within the required tolerances. Contrarily, dimensions created by a set of non-consecutive cuts, such as, the width of the constrainer (50 *μm*), the outer diameter of the actuation unit (200 *μm*), the width of the actuation beam between two adjoining actuation units (25.7 *μm)* were not sufficiently accurate as mentioned before. Although, achieving highest accuracy and precision was never been the objective of this study, some dimensions of the fabricated prototypes were machined within sub-micron accuracy, for example, the width of the tweezing jaws and the length of the constrainer represents feature accuracy of 0.5 *μm* and 0.1 *μm* respectively, mainly due to high positional accuracy of the motion system, proper synchronization of motions, laser on/off events and the desired geometry. Note that the outer diameter of the actuation unit (200 *μm*), the length of the five actuation units (875 *μm*) and the total length of all actuation units and jaws (2150 *μm*), are a combination of several local design elements, and have relatively large geometric deviations, e.g., 6.0 *μm*, 4.7 *μm*, and 11.9 *μm*, respectively. The source of these deviations is the accumulation of dynamic and positional errors during machining of several local design elements.

6. PERFORMANCE TESTING

The performance testing of the microgripper prototypes was carried out using an optical microscope ("Mitutoyo" model 400) and VisionGauge® software. The microgripper was placed under the microscope and DC voltage was applied several times between the anchors. The time-space motions of the microgripper were video recorded on-line and tweezing distances were measured from the recorded images.

Figure 8 shows the typical performance of two microgripper prototypes as a function of tweezing distance in time with respect to the applied voltage and current. Approximately ten tweezing movements were recorded and measured for each of applied current setting. Complete dynamic performance of the nickel-based microgripper was analyzed at six different current levels {0.32 *A*, 0.39 *A*, 0.52 *A*, 0.60 *A*, 0.74 *A*, 0.84 *A*} with corresponded voltages of {1.60V, 1.63V, 1.70V, 1.80V, 1.90V, 2.0V}. Copper-based micro-gripper prototype requires significantly higher electric power and current due to higher electro-conductivity and therefore was tested at five different current levels of {1.63A, 2.05A, 2.65A, 3.1A, 3.4A} with corresponded voltages of {0.70V, 0.78V, 1.10V, 1.51V, 1.59V}. Figure 9 illustrates tweezing motions of the nickel-based and copper-based prototypes before (Figure 9a) and after (Figure 9b) actuation. The nickel-based microgripper was actuated with 1.9 *V*, 0.84 *A*, achieving a tweezing displacement of 32.6 *μm*. Contrarily, the copper-based microgripper was actuated with 1.5 *V*, 3.4 *A*, achieving a tweezing displacement of 15.3 *μm*. More comprehensive results of all performance test experiments are illustrated in Figure 10. It is obvious that tweezing distance increases with the concomitant increase in the applied current until the temperature of the actuation beam reaches its melting point. The maximum tweezing displacement of 33.8 *μm* and 17.2 *μm* was recorded for nickel-based and copper-based microgrippers respectively.

7. SUMMARY and CONCLUSIONS

This work was completed in three logical and interrelated steps – from the conceptual design to the fabrication and performance testing of the electro-thermally driven microgrippers for micromanipulating and microhandling operations in MEMS, biological, medical, chemical and electro-opto-mechanical applications. In the first part, overall design and the design of the actuation unit were developed and discussed in details. As a case study, two microgrippers - copper-based and nickel-based prototypes with overall dimension of 1.4 (L) x 2.8 (W) *mm* were fabricated using a high-precision laser-material removal process. During fabrication, several technical challenges were addressed in order to achieve desired geometrical accuracy and precision. The solution methods allowed fabrication accuracy of several local dimensions with less than one micrometer. The dynamic performance of the fabricated prototypes was studied and compared in terms of achieving maximum tweezing displacement under similar control parameters (ex. voltage and current). The microgrippers exhibited tweezing displacements from 0.8 *μm* to 32.6 *μm* for an applied current variation from 0.32 *A* to 0.84 *A* for nickel-based prototype and tweezing displacements from 3.1 μm to 17.2 μm for copper-based prototype for applied current variation from 1.6 A to 3.4 A. Following conclusions can be drawn from these studies:

1. Design and performance of the individual actuation unit is a key component in the overall performance of the microgripper. A combination of the two thin semi-circular-shaped actuation beams and a wider constrainer between them allowed direct thermal expansion in the desired horizontal direction through non-uniform resistive heating.
2. Complexity in the microgripper design as a combination of the design elements with high dimensional aspect ratios between them lead to agile non-consecutive motions of the XY translational stages during laser fabrication. Therefore, motion system alters its dynamic accuracy due to high inertial forces, and dynamic errors become as comparable to some of the desired feature dimensions. These agile non-consecutive motions were taken into account during toolpath trajectory planning that enabled overall relative accuracy less than 1% for majority of machined dimensions.
3. Synchronization of motions and laser-on/off events in space and time with respect to the desired toolpath trajectory plays a key role in dynamic performance of the entire laser microfabrication process. Therefore, in order to achieve geometrical accuracy and precision less than one micrometer, it is necessary to modify toolpath trajectory with respect to the dynamics of motions while considering the thermodynamics of the laser-material interactions.
4. The nickel-based microgripper prototype has successfully demonstrated the ability to produce higher tweezing displacements (up to 32.6 μm) and higher

displacement-current gradient (up to 34.29 *μm/A*) with lower applied current (0.84 *A*) compared to the copper-based microgripper and a typical response time was 200 *ms* at 1.6 *W* electrical driving power.

5. The developed microgripper prototypes provide an inexpensive, compact solution for micromanipulating and microhandling operations in biological, medical, chemical and electro-opto-mechanical applications.

ACKNOWLEDGEMENTS

This work was conducted under the joint agreement between IMTI-NRC and The University of Western Ontario, London, Ontario, Canada. During the course of this project, the students, Mr. Norman Cheng, Mr. Brandon Hall and Mr. Shiu-Yeung Hui, performed FEA calculations and performance testing, and participated in the laser fabrication experiments. Their assistance and help are appreciated. Thanks are also due to Mr. Mahmud-Ul Islam, Director, Production Technology Research, and Prof. Brian Thompson, NSERC-GM of Canada Chair of Engineering in Design and Innovation, UWO, for their continued support in this work. The authors also appreciate the assistance of Mr. Keddie Brown, Mr. Hugo Reshef and Mr. Craig Dinkel, for their help in performing the laser fabrication experiments.

REFERENCES

1. M.J. Madou, "*Fundamentals of Microfabrication: The Science of Miniaturization*," CRC Press, New York, NY (2002).

2. T.-R. Hsu, "*MEMS & MICROSYSTEMS: Design and Manufacture*," McGraw-Hill, New York, NY (2002).
3. "*MEMS and MOEMS: Technology and Application*," P. Rai-Choudhury, Ed., SPIE Press, Bellingham, WA (2000).
4. W.C. Tang, T.U. Chong, H. Nguyen, and R.T. Howe, "Laterally driven polysilicon resonant microstructures," *Sensors and Actuators A*, **20**, 25-32 (1989).
5. C.J.Kim, A.P. Pisano, and R.S. Muller, "Silicon-processed overhanging micro-gripper", *Journal of Electromechanical Systems*, **1**(1), 31-35 (1992).
6. M. Esashi, M. Yamaguchi, S. Kawamura, and K. Minami, "Control of distributed electrostatic microstructures," *Journal of Micromechanics and Microengineering*, **3**, 90 – 95 (1993).
7. A. Desai, S.-W. Lee, and Y.-C. Tai, "A MEMS electrostatic particle transportation system", *Sensors and Actuators*, **73**, 37-44 (1999).
8. B.E. Volland, H. Heerlein, and I.W. Rangelow, "Electrostatically driven microgripper", *Microelectronic Engineering*, **61-62**, 1015-1023 (2002).
9. W.A. Moussa, H. Ahmed, and M. Moussa, "Investigating the reliability of electrostatic comb-drive actuators used in microfluidic and space systems using finite element analysis," Can. J. Elect. Comput. Eng., **27**(4), 195-200 (2002).
10. H. Guckel, J. Klein, T. Christenson, K. Skrobis, M. Laudon, and E.G. Lovel, "Thermo-magnetic metal flexure actuators", Technical Digest, 1992 Solid-State Sensors and Actuators Workshop, Hilton Head, SC, USA, 73-75 (1992).
11. J. Li and G.K. Ananthasuresh, "A quality study on the excimer laser micromachining of electro-thermal-compliant microdevices", *Journal of Micromechanics and Microengineering*, **11**, 38 – 47 (2001).

12. N.D. Mankame and G.K. Ananthasuresh, "Comprehensive thermal modelling and characterization of an electro-thermal-compliant microactuator", *Journal of Micromechanics and Microengineering*, **11**, 452 – 462 (2001).

13. L.L. Chu and Y.B. Gianchandani, "A micromachined 2D positioner with electrothermal actuation and sub-nanometer capacitive sensing", *Journal of Micromechanics and Microengineering*, **13**, 279 – 285 (2003).

14. H. Sehr, A. G. R. Evans, A. Brunnschweiler, G.J. Ensell, and T.E.G. Niblock, "Fabrication and Test of Thermal Vertical Bimorph Actuators for Movement in Wafer Plane," *Journal of Micromechanics and Microengineering*, **11**, 306 – 310 (2001).

15. D. Yan, A. Khajepour, and R. Mansour, "Modelling of two-hot-arm horizontal thermal actuator," *Journal of Micromechanics and Microengineering*, **13**, 312 – 322 (2003).

16. C.-P. Hsu, W.-C. Tai, and W. Hsu, "Design and Analysis of an Electro-Thermally Driven Long-Stretch Micro Drive with Cascaded Structure," *Proceedings of the ASME International Mechanical Engineering Congress*, New Orleans, Louisiana, USA, 235 – 240 (2002).

17. E.V. Bordatchev, S.K. Nikumb, and W.-S. Hsu, "Fabrication of Long-Stretch Microdrive for MEMS Applications by Ultra Precision Laser Micromachining," *Proceedings of the Canada-Taiwan Workshop on Advanced Manufacturing Technologies*, London, Ontario, Canada, 243 – 251 (2002).

18. M. Kohl, B. Krevet, and E. Just, "SMA microgripper system," *Sensors and Actuators A*, **97-98**, 646-652 (2002).

19. M. Kohl, E. Just, W. Pfleging, and S. Miyazaki, "SMA microgripper with integrated antagonism," *Sensors and Actuators A*, **83**, 208-213 (2000).

20. J.P. Tan, W.M. Huang, X.Y. Gao, J.H. Yeo, and J.M. Miao, "NiTi shape memory

alloy thin film based microgripper," *Processing of SPIE*, **4234**, 106-113 (2001).

21. W.M. Huang, J.P. Tan, X.Y. Gao, and J.H. Yeo, "Design, testing, and simulation of NiTi shape-memory-alloy thin-film-based microgrippers," *Journal of Microlithography, Microfabrication, and Microsystems*," **2**(3), 185-190 (2003).
22. I. Roch, Ph. Bidaud, D. Collard, and L. Buchaillot, "Fabrication and characterization of an SU-8 gripper actuated by a shape memory alloy thin film," *Journal of Micromechanics and Microengineering*," **13**, 330-336 (2003).
23. M. Sakata, S. Wakabayashi, H. Goto, H. Totani, M. Takeuchi, and T. Yada, "Sputtered high d31 coefficient PZT thin film for microactuators," *Proc. IEEE Micro Electro Mechanical System*, San Diego, CA, 263-266 (1996).
24. K.G. Brooks, M. Reaney, T. Maeder, and N. Setter, "Processing sol-gel PZT films for microactuators," *Proc. Electroceramics IV Conf. Electronic Ceramics and Applications*, Aachen, Germany, 407-410 (1994).
25. G. Preu, A. Wolff, D. Cramer, and U. Bast, " Microstructuring of piezoelectric ceramic," *Proc. 2nd European Ceramic Society Conference*, Augsburg, Germany, 2005-2009 (1991).
26. G. Thornell, L. Klintberg, T. Laurell, J. Nilsson, and S. Johansson, "Desktop microfabrication - initial experiments with a piezoelectric," *J. Micromech. Microeng.*, **9**, 434-37 (1999).
27. "*LIA Handbook of Laser Materials Processing*," Editor-in-Chief: J.F. Ready, LIA Press, Orlando, FL, (2001)
28. A. Braun and K. Zimmer, "Fabrication of MEMS structures by laser machining", *Proceedings of SPIE*, **4236**, 213-221 (2001).
29. E.V. Bordatchev and S.K. Nikumb, "An Experimental Study and Statistical Analysis

of the Effect of Laser Pulse Energy on the Geometric Quality during Laser Precision Machining", *Machining Science and Technology: An International Journal*, 7(1), 83-104 (2003).

30. E.V. Bordatchev and S.K. Nikumb, "Laser material-removal process as a subject of automatic control," *Proceedings of the ASPE 14th Annual Meeting*, Monterey, CA, 236-239 (1999)
31. S.R. Vatsya, E.V. Bordatchev, and S.K. Nikumb, "Geometrical Modeling of Surface Profile Formation during Laser Ablation of Materials", *Journal of Applied Physics*, **93**(12), 9753-9759 (2003).
32. E.V. Bordatchev and S.K. Nikumb, "Dynamic performance of high precision laser micromachining systems", *Proceedings of the 2000 NSF Design & Manufacturing Research Conference*, Vancouver, BC, Canada, (2000).
33. E. V. Bordatchev and S.K. Nikumb, "Improving Geometric Quality of Laser Micromachined Parts using High-Precision Motion System Dynamic Performance Analysis," *Proceedings of the 3rd World Manufacturing Congress*, Rochester, NY, Paper # 1924-103 (2002).
34. E.V. Bordatchev, "Analysis and Mapping of the Dynamic Performance of High-Precision Motion Systems." In book: "*Integrated Design and Manufacturing in Mechanical Engineering*". Kluwer Academic Publishers, Norwell, USA, 255-262 (2002).
35. B.F. Yousef, G.K. Knopf, E.V. Bordatchev, and S.K. Nikumb, "Neural Network Modeling and Analysis of the Material Removal Process during Laser Machining", The International Journal of Advanced Manufacturing Technology, **22**, 41-53 (2003).
36. E.V. Bordatchev and S.K. Nikumb, "Informational Properties of Surface Acoustic

Waves Generated by Laser-Material Interactions during Laser Precision Machining", *Measurement Science and Technology Journal*, **13**(6), 836-845 (2002).

37. E. V. Bordatchev and S.K. Nikumb, "Geometric Quality Analysis and Process Control for Ultra-Precision Laser Micromachining," *Proceedings of the ASPE 16th Annual Meeting*, Arlington, VA, 281-284 (2001).

List of table headings

Table 1. Geometry evaluation

Table 1. Geometry evaluation

Desired dimension, μm	Machined dimensions, μm	Absolute accuracy, μm	Relative accuracy, %	Type of operation
25.7	27.1	1.4	5.45	non-consecutive cuts
50.0	47.9	2.1	4.20	non-consecutive cuts
50.0	52.7	2.7	5.40	non-consecutive cuts
50.0	49.5	0.5	1.00	consecutive cuts
100.0	97.4	2.6	2.60	consecutive cuts
150.0	149.9	0.1	0.07	single cut
200.0	206.0	6.0	3.00	non-consecutive cuts
200.0	201.2	1.2	0.60	consecutive cuts
525.0	528.5	3.5	0.67	consecutive cuts
850.0	849.4	0.6	0.07	consecutive cuts
875.0	878.2	3.2	0.37	consecutive cuts
875.0	879.7	4.7	0.54	consecutive cuts
2150.0	2161.9	11.9	0.55	consecutive cuts

List of figure captions

Figure 1. Paradigm of the micro-gripper development framework

Figure 2. Conceptual design of the microgripper

Figure 3. Schematic diagram of the basic actuation unit

Figure 4. Geometrical design (dimensions in *μm*)

Figure 5. Schematic of the laser microfabrication system

Figure 6. Challenges in laser microfabrication of the microgripper prototype

Figure 7. Fabricated nickel-based microgripper prototype (dimensions in *μm*)

Figure 8. Typical performance test results of the nickel-based and copper-based microgripper prototypes

Figure 9. Actual motions of the copper-based and nickel-based microgripper prototypes

Figure 10. Comparison of performances of copper-based and nickel-based microgripper prototypes

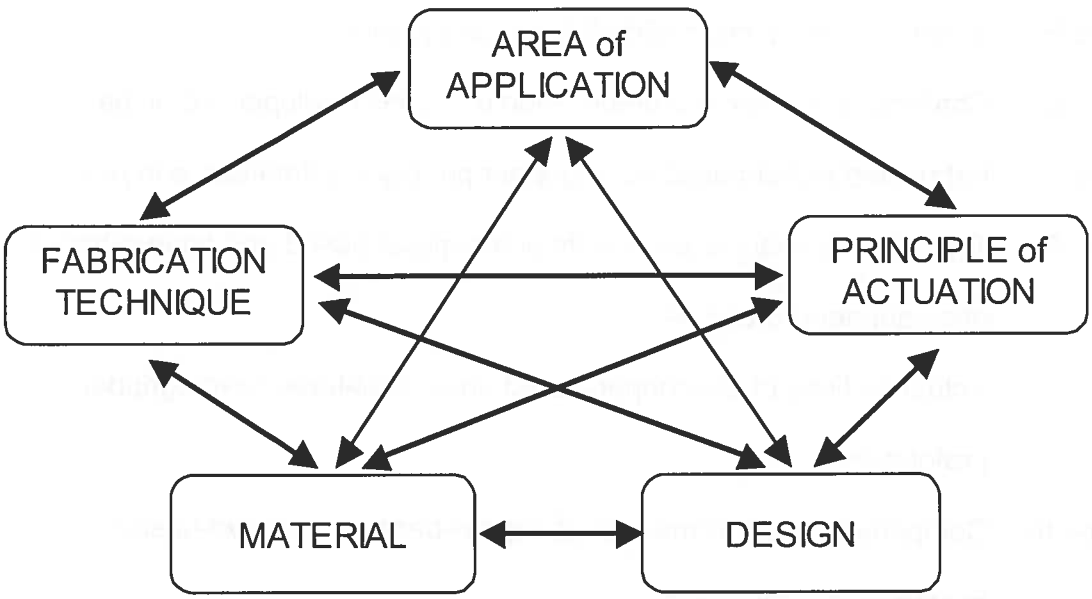

Figure 1. Paradigm of the micro-gripper development framework.

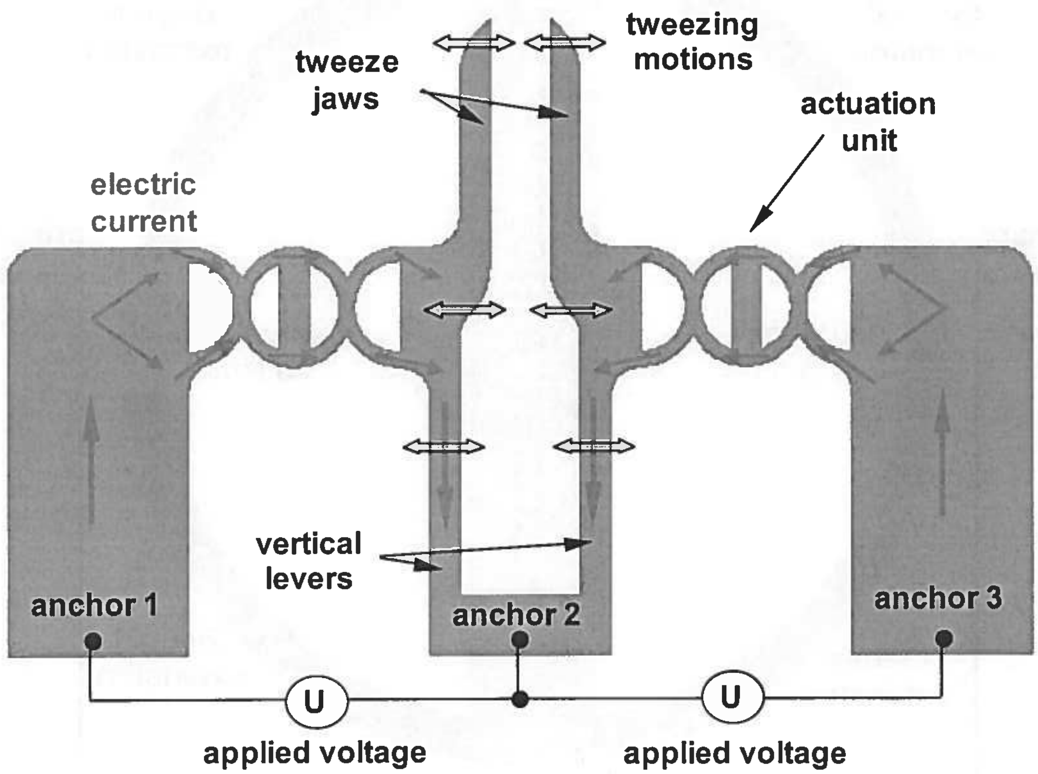

Figure 2. Conceptual design of the microgripper.

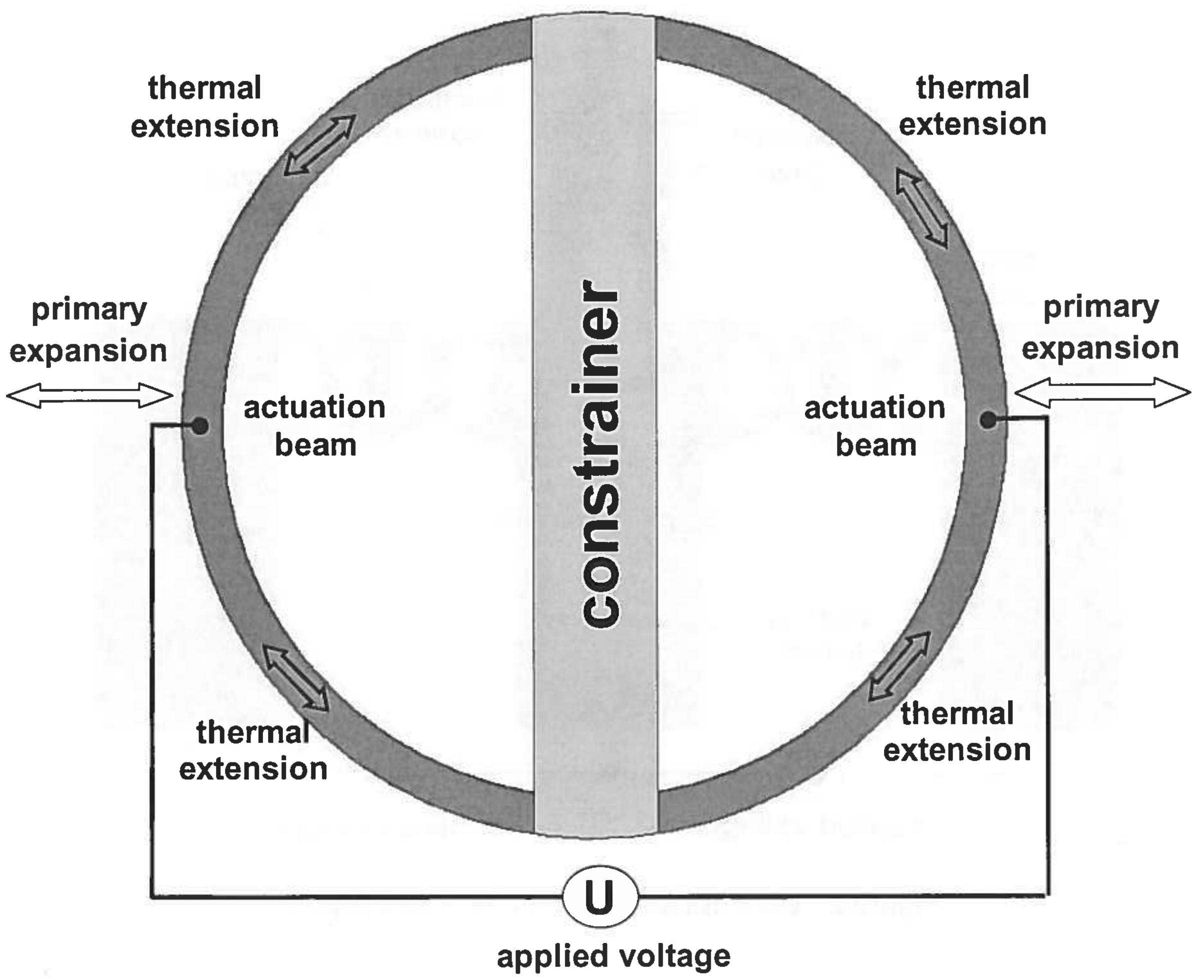

Figure 3. Schematic diagram of the basic actuation unit.

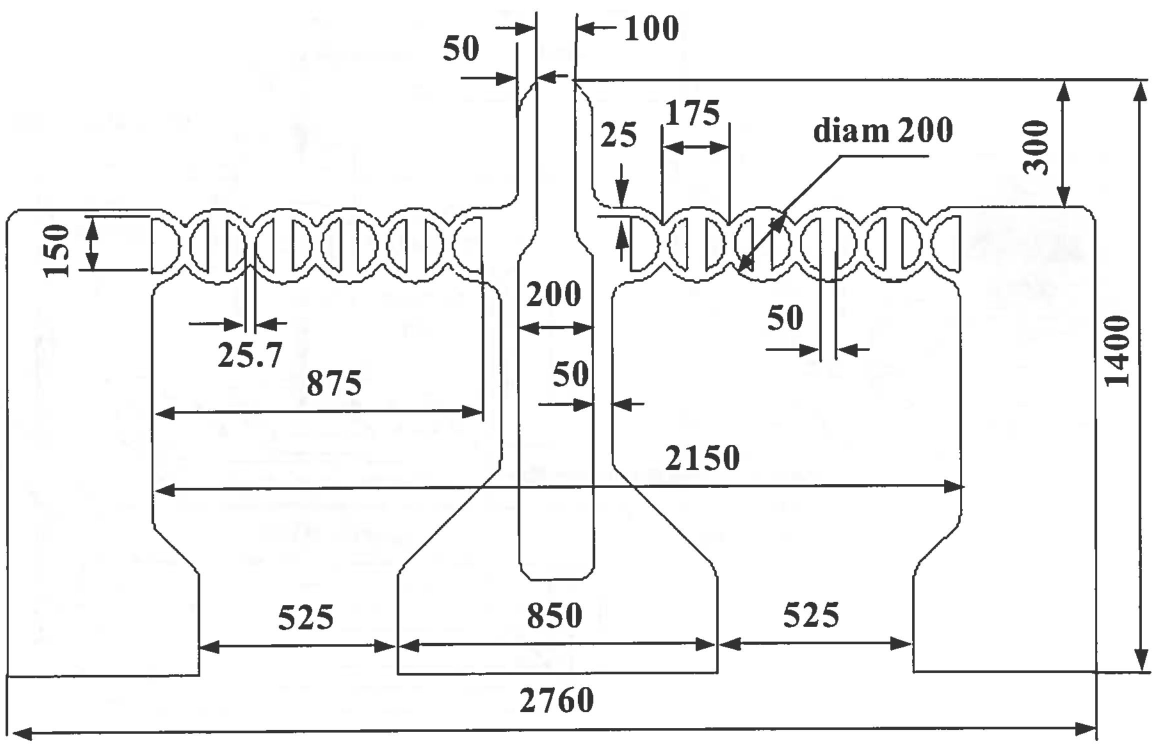

Figure 4. Geometrical design (dimensions in μm).

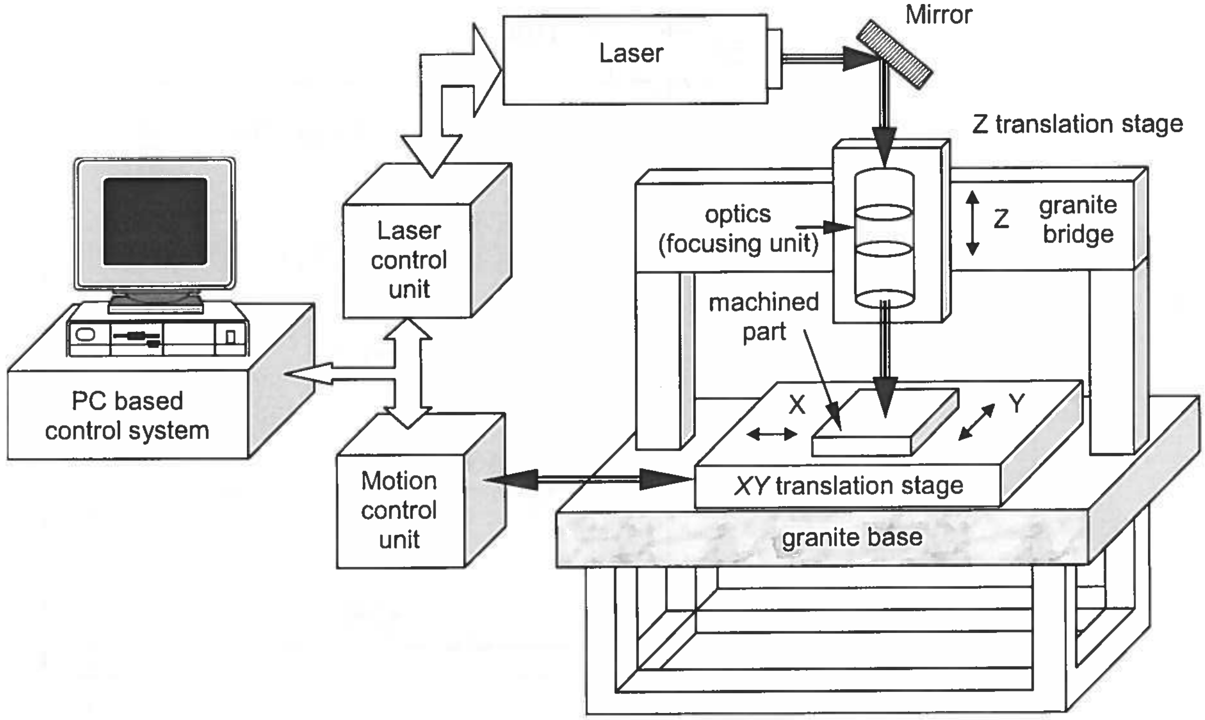

Figure 5. Schematic of the laser microfabrication system.

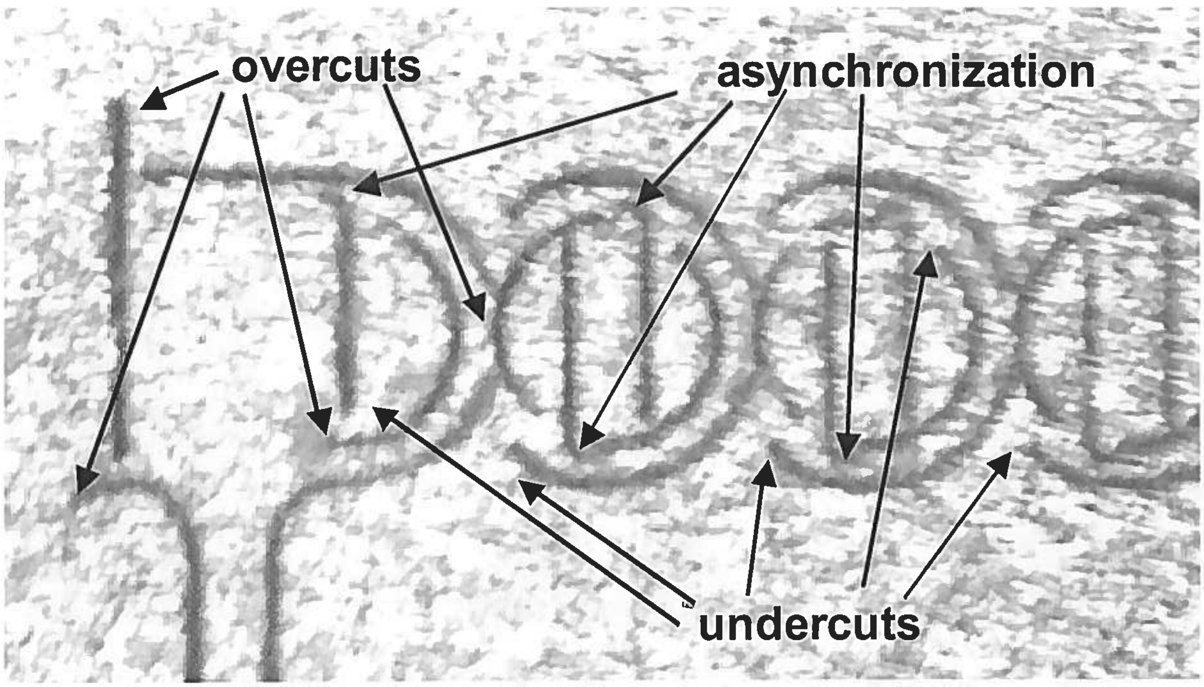

Figure. 6. Challenges in laser microfabrication of the microgripper prototype.

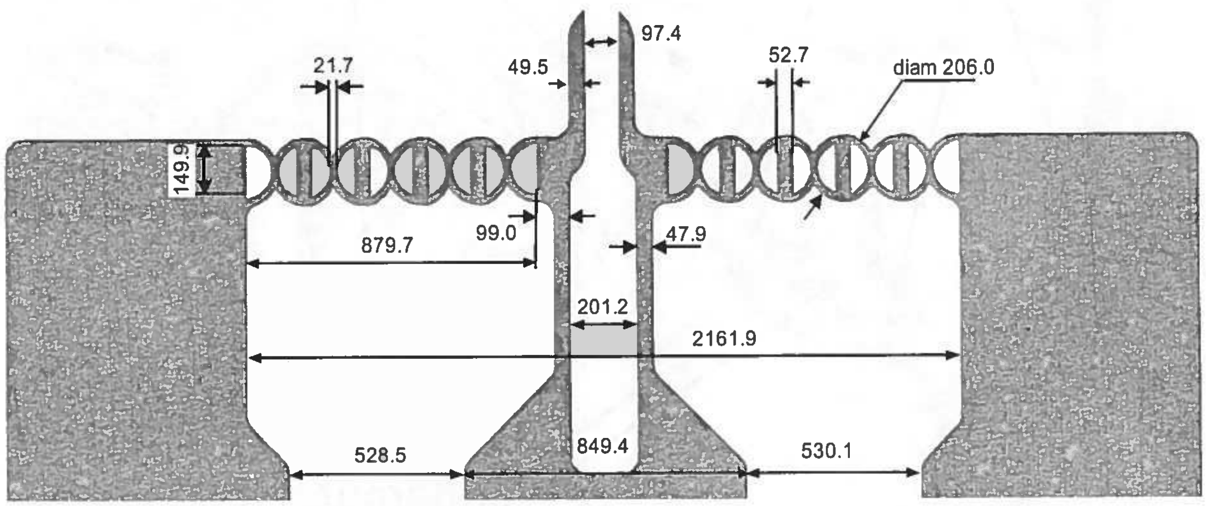

Figure 7. Fabricated nickel-based microgripper prototype (dimensions in μm).

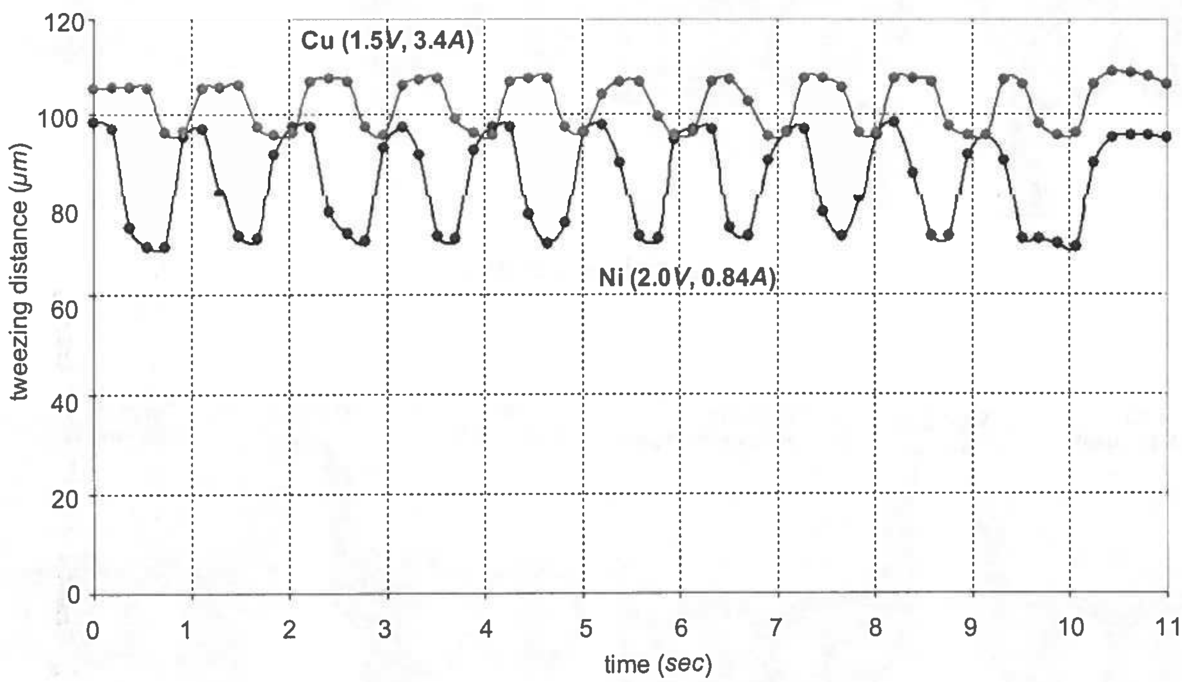

Figure 8. Typical performance test results of the nickel-based and copper-based microgripper prototypes.

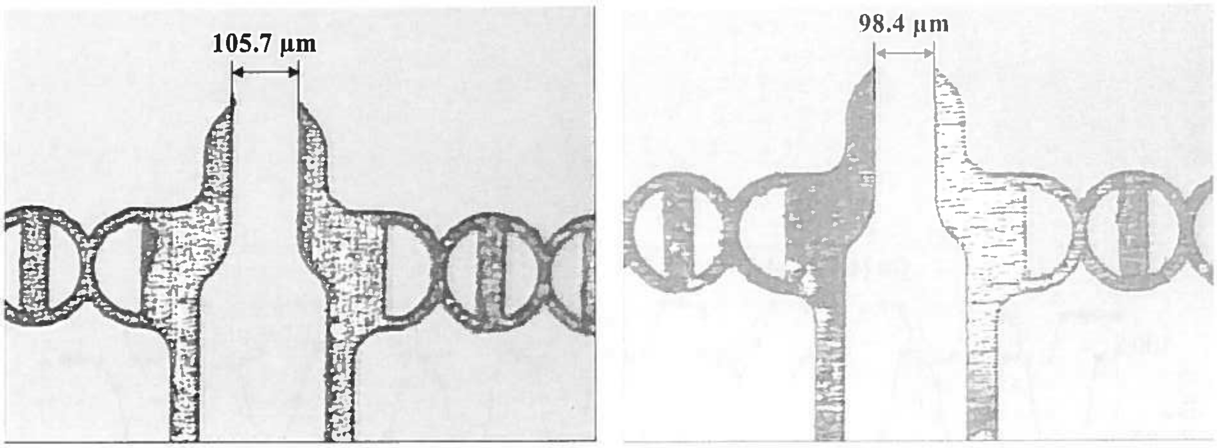

(a) before actuation

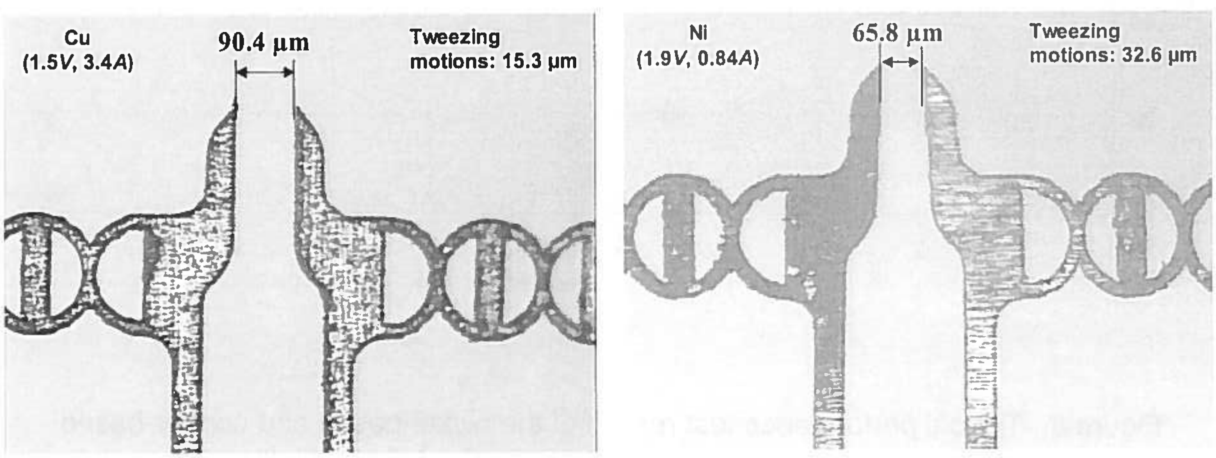

(b) after actuation

Figure 9. Actual motions of the copper-based and nickel-based microgripper prototypes.

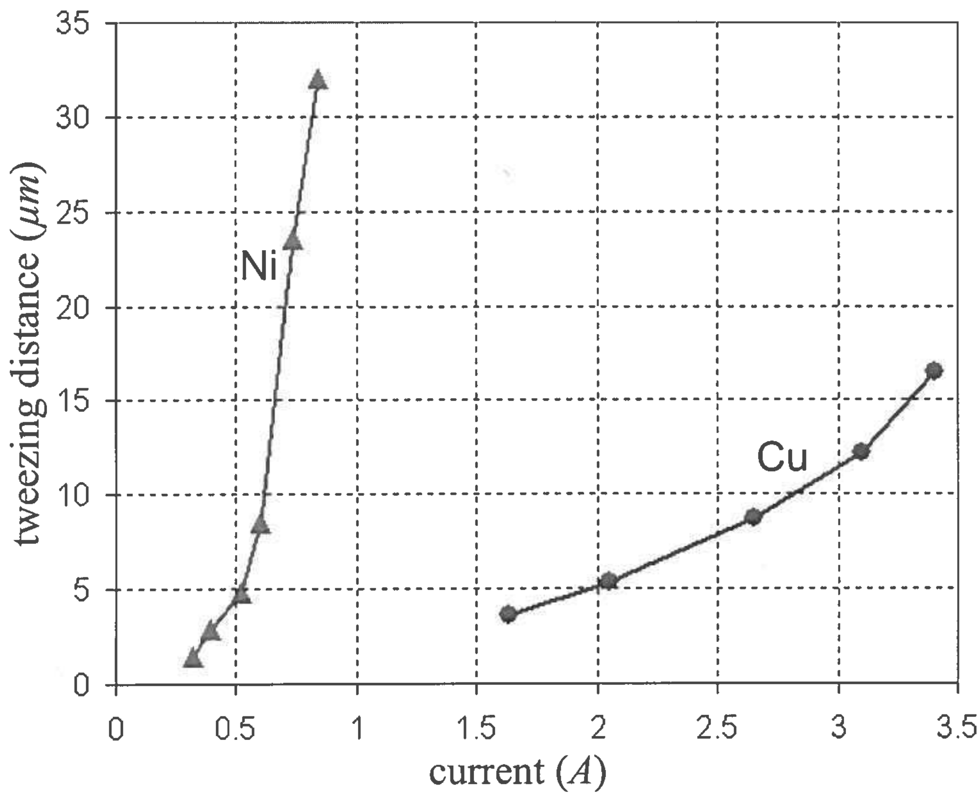

Figure 10. Comparison of performances of copper-based and nickel-based microgripper prototypes.